*Bull. Mater. Sci.*, Vol. 40, No. 6, October 2017, pp. 1225–1230
DOI 10.1007/s12034-017-1450-9



# Thickness and photocatalytic activity relation in $TiO_2$:N films grown by atomic layer deposition with methylene-blue and *E. coli* bacteria

**M M M CONTRERAS TURRUBIARTES[1], E LÓPEZ LUNA[1], J L ENRIQUEZ-CARREJO[2], A PEDROZA RODRIGUEZ[3], J C SALCEDO REYES[3], M A VIDAL BORBOLLA[1] and P G MANI-GONZALEZ[2,*]**

[1]Coordinacion para la Innovación y Aplicación de la Ciencia y la Tecnología, Universidad Autónoma de San Luis Potosí, Sierra Leona #550, Lomas 2a. Sección, San Luis Potosí, Mexico
[2]Departamento de Física y Matemáticas, Instituto de Ingeniería y Tecnología, Universidad Autónoma de Ciudad Juárez, Ave. Del Charro 450, Cd., C.P. 32310 Juárez, Chihuahua, Mexico
[3]Pontificia Universidad Javeriana, Carrera 7 #40-62, Bogotá, Colombia
*Author for correspondence (pierre.mani@uacj.mx)

MS received 22 November 2016; accepted 25 January 2017; published online 15 September 2017

**Abstract.** This study presents an analysis of the photocatalytic efficiency in $TiO_2$:N thin films grown by atomic layer deposition related to the film thickness. The nitriding process was carried out with nitrogen plasma by molecular nitrogen decomposition after $TiO_2$ deposition. The study was performed using the time-dependent degradation of colour units for methylene-blue solutions and inactivation percentages for *Escherichia coli* bacteria, for potential applications in sewage purification. To determine the optoelectronic properties of the films, the optical, structural, surface and thickness characterizations were carried out by photoluminescence, Raman spectroscopy, atomic force microscopy and scanning electron microscopy, respectively.

**Keywords.** Photocatalytic; atomic layer deposition; anatase phase; photoluminescence; degradation; inactivation.

## 1. Introduction

At present, there has been an increase in research related to heterogeneous photocatalysis by titanium dioxide ($TiO_2$) due to the existing need of efficiency increase in wastewater purification processes [1,2]. As it is known, $TiO_2$, in the presence of ultra-violet radiation (UV), has the ability to induce oxidation and reduction reactions of the oxygen molecules adsorbed on the semiconductor/medium interface producing a biocidal and sterilizer effect [3–5]. Other narrowband semiconductors have been studied, mainly CdS and CdSe, observing photo-oxidation processes on the surface [6,7]. Nonetheless, the highest photocatalytic efficiencies were obtained with $TiO_2$. $TiO_2$ is a low-cost material, non-toxic and biologically inert [8–10]. The photocatalytic properties in $TiO_2$ were usually analysed in films formed from a titanium powder suspension (in anatase phase). $TiO_2$ thin films can be grown by other methods such as sol–gel. By using this method, the films usually have different phases [11–13]. Another option is sputtering; the literature shows that amorphous and polycrystalline films with a big range in roughness have been grown using this technique [14–16]. Films with a good homogeneity have been produced by spray pyrolysis technique, but require high temperatures compared to other methods [17–19]. Atomic layer deposition (ALD) offers the advantage that films with a determined structure, high homogeneity and low roughness can be obtained at a low temperature [20,21].

ALD is a technique which operates with materials in the gaseous phase. With the use of this deposition method it is possible to grow films in a layer by layer approach at low temperatures. The thin films obtained by this method have high homogeneity, good stoichiometry and exhibit high substrate adhesion. Also, ALD allows deposition of films with defined thickness ensuring repeatability of experiments [7,22–24]. At present, these characteristics have made ALD as one of the techniques with most chances to enhance photocatalytic systems such as $TiO_2$ [25].

In ALD, precursor gases are introduced alternately into the reaction chamber in such way that the gas reacts with the surface of the substrate in each pulse; in this way a monolayer of the desired material is created. Substrate temperature and precursors promote adherence to the atomic layer. The reaction chamber is purged with an inert gas which removes the excess precursor gas. This method allows an optimal control of both composition and growth rate [26]; it also enables the production of pure or doped $TiO_2$ thin films on different substrates such as glass or silicon with potential applications in the field of heterogeneous catalysis [27].

The aim of this study is to analyse the photocatalytic efficiency in $TiO_2$ films as a function of thickness and nitrogen incorporation. The incorporation of nitrogen into $TiO_2$ can shift light absorption near the visible region, increasing the photocatalytic activity by decreasing the bandgap or creating N-induced mid-gap levels [28]. Methylene blue is a major component in wastewater, mainly because of its use in the textile industry.

*Escherichia coli* (*E. coli*) is a notable bacterium that can be found in the human intestine. Most of the types of *E. coli* are inoffensive for humans. However, some other kinds such as enterohemorrhagic *E. coli* can cause death. It can be transmitted to humans by contaminated food like raw meat and vegetables [29]. Some methods such as $TiO_2$ particles in solution have been used to damage *E. coli* bacteria [30].

## 2. Materials and methods

The films were grown on intrinsic silicon substrates (100). Cambridge Nanotech Savannah ALD 200 equipment was used for this task. Titanium isopropoxide ($Ti(Oi\text{-}Pr)_4$) and water ($H_2O$) were used as titanium source and oxygen source, respectively. The film thickness was varied with the number of cycles: 200, 300, 400 and 500 cycles. The film surface roughness was measured using an atomic force microscopy (AFM) microscope SPM Solver NEXT NT-MDT in tapping mode. Raman spectroscopy was performed using a green laser (532 nm) source.

The nitriding process was carried out for all films in a vacuum chamber. The working pressure was $10^{-8}$ Torr. The chamber was adapted with a nitrogen plasma source which uses radiofrequency for molecular nitrogen decomposition. The $TiO_2$ film was exposed to the plasma for 30 min at 500°C. The aim of this process is to change the bandgap of $TiO_2$ due to the creation of intermediate transition levels and to obtain properties as photocatalytic efficiency.

Photoluminescence (PL) characterization was accomplished using a UV laser (325 nm) at 10 K. The photocatalytic efficiency characterization was carried out using a mixture of methylene blue at 5 ppm. This mixture was irradiated using a UV lamp ($\lambda = 325$ nm) at 0.16 mW. The films were immersed in a 10 ml mixture of methylene blue. For quantifying the degradation of methylene blue, transmittance spectra were used in all samples. The spectra were obtained using a Perkin Elmer Lambda 25 spectrometer.

Inactivation test of *E. coli* bacteria was made using 5 ml of peptone water solution as a buffer. Then, all samples were irradiated for 30 min with UV light ($\lambda = 254$ nm). Post-irradiation each solution sample was cultivated using the seeding method by microdroplet for calculation of the inactivation percentage. The surface area of the film was 1 $mm^2$.

The following nomenclature was used in this work: 200, 300, 400 and 500 (number of ALD cycles), WON (without nitrogen), N (with nitrogen).

## 3. Results

### 3.1 *$TiO_2$ films characterization*

Figure 1 presents the images obtained by AFM for 200 and 500 ALD cycles. Film roughness increases with number of ALD cycles. It is possible to observe some structures at the surface of thicker films. This can be related to the growth process of $TiO_2$, specifically to the arrangement of the atomic layers according to the unit cell of the $TiO_2$ phase. This is essential for photocatalytic processes, which is associated with flat films [31]. Also, it can be seen that roughness decreases after the nitriding process, which is attributable to the temperature in the vacuum chamber. This nitriding process changes the structure associated with oxygen defects.

The PL spectra for samples without nitrogen are shown in figure 2 for (a) 200, (b) 300, (c) 400 and (d) 500 ALD cycles. Based on the low noise and the position of the energy peaks in the spectra, it is possible to observe that the films exhibit anatase phase. The energy peaks are related to colour centres in $TiO_2$ and have been reported in the literature; also, these peaks suggest oxygen vacancies. Some studies show that the photocatalytic process occurs in those sites [31,32]. A peak close to 2.3 eV is present in all samples; this is related to oxygen vacancies in the anatase phase of $TiO_2$.

In spectrum (a), deconvolutions (dotted lines) show a peak close to 2.9 eV which is not present in the other spectra and is related to defects in $TiO_2$. In addition, spectra (c) and (d) show a peak close to 2.1 eV, this peak is related to defects in anatase phase of $TiO_2$ [33,34].

The spectra of the films with nitrogen are shown in figure 3 for (a) 200 and (b) 500 ALD cycles. The shape of the spectra is associated with $TiO_2$. New peaks related to colour centres appear due to the nitriding process.

The spectra show 4 peaks at 2.05, 2.3, 2.55 and 2.93 eV. The first two peaks are related to N–Ti–O defects and the other two peaks correspond to oxygen vacancies. All peaks are related to the anatase phase of $TiO_2$ [32,33].

Additionally, the shape of the PL peaks changes after the nitriding process. These changes are evidence of the nitrogen incorporation [33,34]. Some authors associate these peaks to the presence of defects of N–Ti–O type and oxygen vacancies as a consequence of the nitriding process. Also, it has been demonstrated that these defects contribute to the absorption of light in a wider range [32,34,35]. This can be a factor to increase the photocatalytic efficiency.

The Raman spectra of films are shown in figure 4: (a) 500WON and (b) 200WON. The vibrations at 170 and 643 $cm^{-1}$ correspond to $E_g$ mode, while the one at 384 $cm^{-1}$ corresponds to $B_{1g}$. These peaks correspond to the anatase phase of $TiO_2$ [35,36]. In spectrum (b), it is not possible to observe the mentioned vibrational modes because its thickness was too small for the equipment capability. The peak close to 520 $cm^{-1}$ is due to the Si(100) substrate. These results together with the PL ones show that the $TiO_2$ films exhibit the anatase phase.

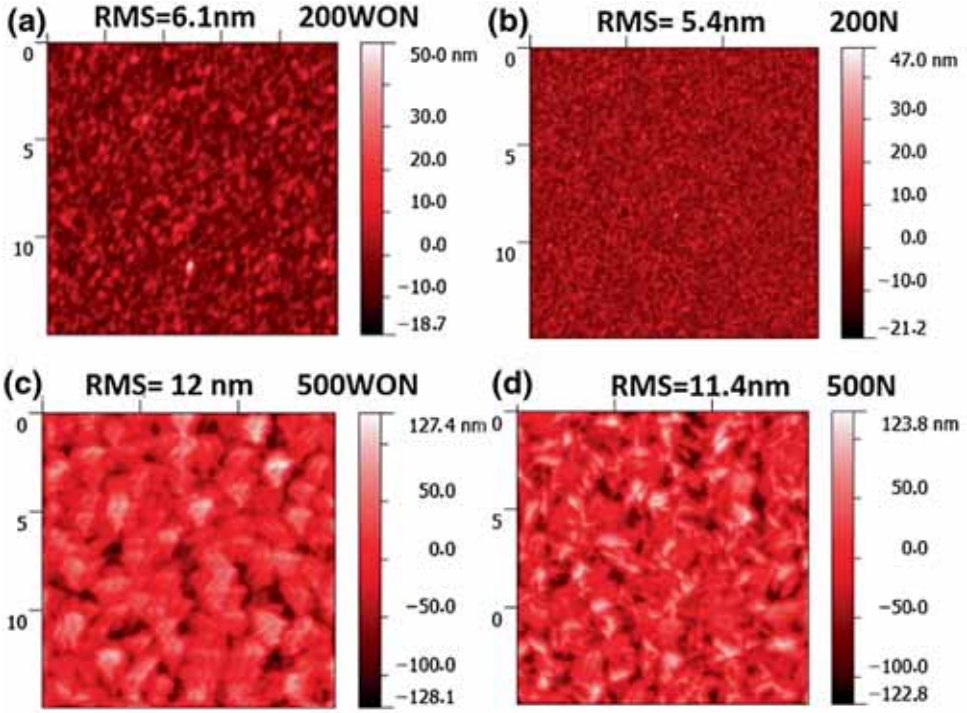


**Figure 1.** Images of AFM for the $TiO_2$ thin films: (**a**) 200WON, (**b**) 200N, (**c**) 500WON and (**d**) 500N.

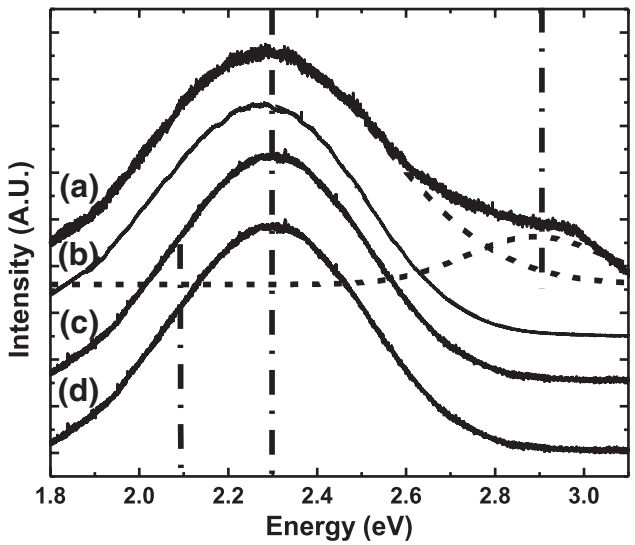


**Figure 2.** Photoluminescence spectra of $TiO_2$ (WON) thin films: (**a**) 200, (**b**) 300, (**c**) 400 and (**d**) 500 ALD cycles.

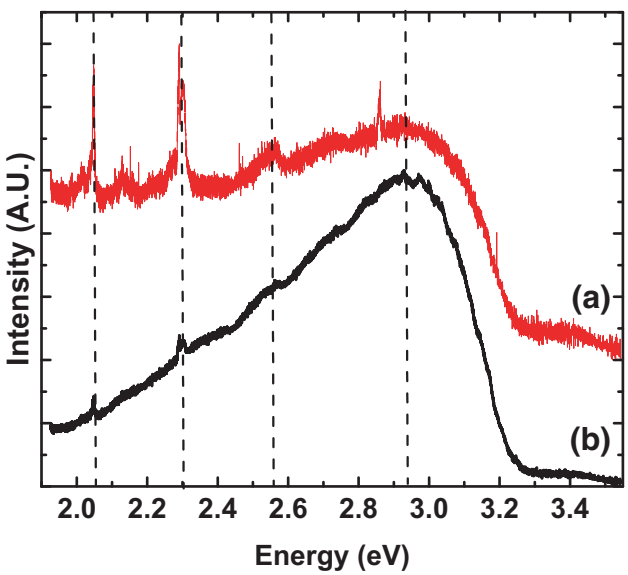


**Figure 3.** Photoluminescence spectra of $TiO_2$:N thin films: (**a**) 200 and (**b**) 500 ALD cycles.

Table 1 presents film thickness values. These measurements were made by scanning electron microscopy (SEM). Figure 5 shows the cross-section of the 200N film.

### 3.2 *Photocatalysis activity test*

The methylene blue solution with the $TiO_2$ films immersed in it was irradiated with UV light for 5 h. After irradiation, the films were removed from the solution and the transmission spectra of the solution were obtained, then the degradation of methylene blue was analysed. Figure 6 shows the spectra of the solutions containing films before (a) and after (b) nitriding process. The spectra of water and methylene blue were obtained and used as a reference.

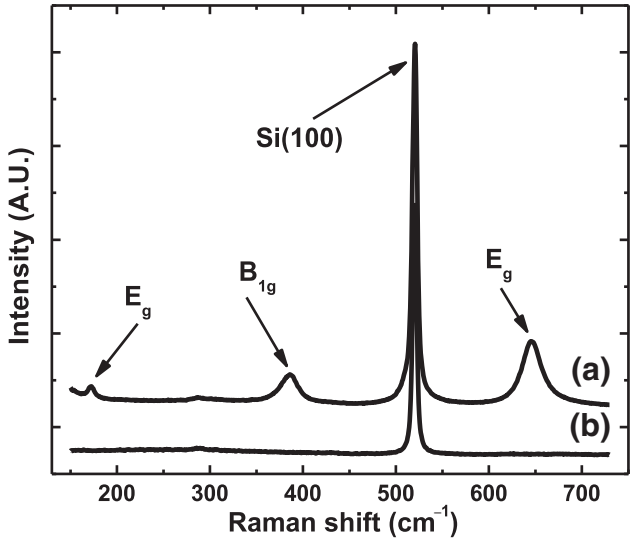


**Figure 4.** (**a**) Raman spectrum of $TiO_2$ 500WON showing the $E_g$ and $B_{1g}$ vibrational modes corresponding to the anatase phase. (**b**) Raman spectrum of $TiO_2$ 200WON, here the $E_g$ and $B_{1g}$ modes are not visible due to the small film thickness.

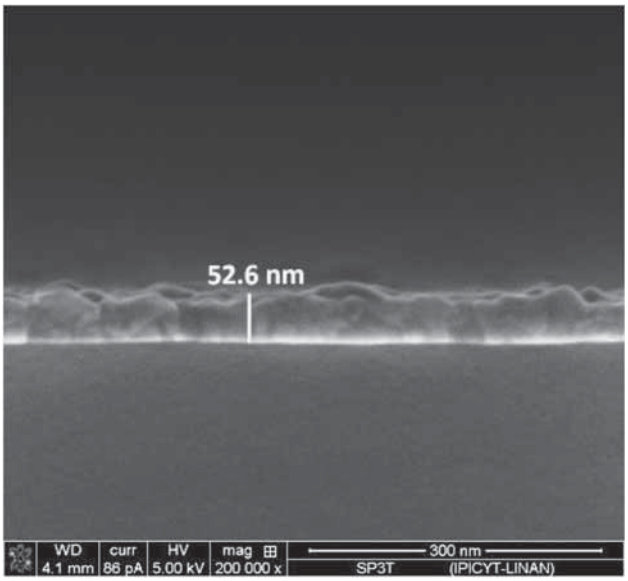


**Figure 5.** SEM image of 200N ALD cycles sample showing film thickness.

**Table 1.** Thickness and degradation percentages of methylene blue for different $TiO_2$ thin films.

| Sample | Thickness (nm) | Degradation (%) |
|---|---|---|
| 200N | 52.6 | 59.3 |
| 200WON | 52.6 | 53.8 |
| 300N | 78.9 | 55.7 |
| 300WON | 78.9 | 52.4 |
| 400N | 105.2 | 54.6 |
| 400WON | 105.2 | 50.7 |
| 500N | 131.5 | 51.1 |
| 500WON | 131.5 | 48.3 |

The upper signal is the buffer reference (water) for the measurements. Spectra in (a) show that the 200WON solution transmittance is higher than the methylene blue due to suspended particles. Spectra in (b) indicate that the 200N solution transmittance is higher than the one for the sample without the nitriding process. This supports the results from PL about the relation to N–Ti–O defects. Based on the intensity of each transmission spectra, the degradation percentages were calculated considering water as reference for a degradation of 100%. Table 1 shows the degradation percentages that correspond to each film-solution after UV light exposure for 5 h. The results indicate that the degradation percentage decreases with the number of ALD cycles independently of the nitriding process. Samples with nitriding process show better efficiency for photocatalytic applications. Figure 7 shows the degradation percentage as a function of time.

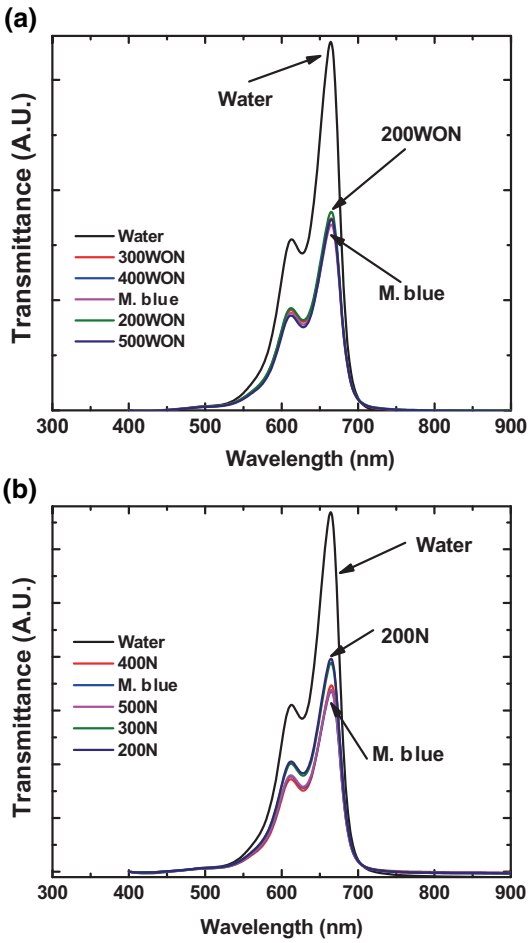


**Figure 6.** Transmission spectra showing the degradation of methylene blue by $TiO_2$ for 5 h. (**a**) Solutions with films-WON and (**b**) solutions with films-N.

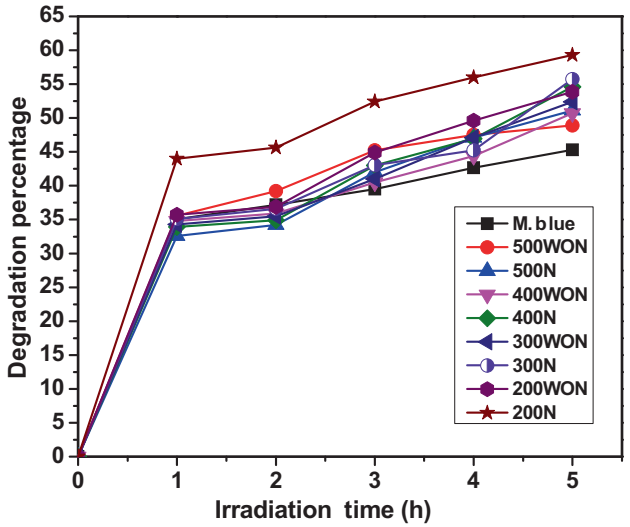


**Figure 7.** Schematic comparison of the degradation percentage of methylene blue for different $TiO_2$ films grown by ALD.

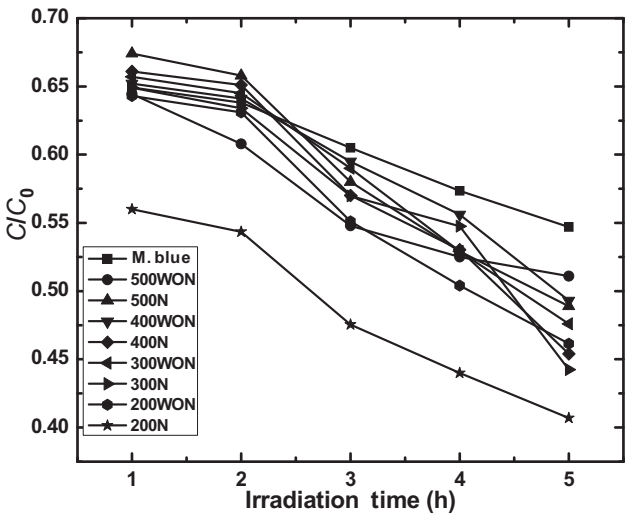


**Figure 8.** Schematic comparison of the ratios $C/C_0$ for the concentration of methylene blue for different $TiO_2$ films grown by ALD.

Figure 8 shows the concentration of methylene blue to initial concentration ratios as functions of time. The 200N sample shows the highest degradation with respect to other samples. These data support the PL and Raman results about the presence of the anatase phase. The existence of oxygen vacancies enhances the photocatalytic activity.

The *E. coli* inactivation results are presented in figure 9. The microdroplet seed method was used to count the number of colony-forming units and to calculate the *E. coli* inactivation percentage [34]. The samples with the highest *E. coli* inactivation percentage were $TiO_2$ films with nitrogen and 200 ALD cycles. Also, it can be seen that the films subjected to nitriding present higher inactivation compared to films of

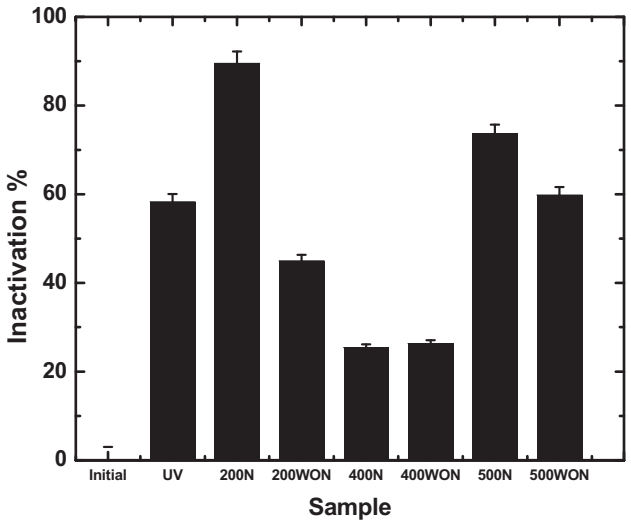


**Figure 9.** Inactivation percentage for *E. coli* by $TiO_2$ films after 30 min of exposition to UV light. The accuracy is ±3%.

only $TiO_2$. In particular, the 200N sample showed the higher inactivation percentage for *E. coli*.

Additional results for inactivation of *E. coli* using $TiO_2$ nanoparticles were reported by others, who obtained an inactivation of 90% after a few hours of UV irradiation [37,38]. Others obtained an inactivation of 85% using $TiO_2$-doped films deposited by sol–gel after an hour of UV irradiation [39].

## 4. Discussion

It was evident that the nitriding process modified the degradation of methylene blue and the inactivation of *E. coli*. This dependence is related to the existence of oxygen vacancies and N–Ti–O type defects. The 200N sample showed the highest degradation rate. Also, it was possible to conclude that degradation is related to film thickness. This could be due to the hole–electron pair generation and their mobility. So, the smaller the thickness the higher the degradation of methylene blue.

The incorporation of nitrogen into the $TiO_2$ films caused a shift in the PL spectra; therefore, the optical properties of the films were altered. The 200N sample has a higher *E. coli* inactivation efficiency. This could be because the hole–electron pairs move to the surface of the film and then react with the cellular membrane braking it.

## Acknowledgements

This project was supported by Colombia–Mexico funding. We would like to thank Universidad Autónoma de San Luis Potosí, Universidad Autónoma de Ciudad Juárez, México and

Pontificia Universidad Javeriana de Bogota, Colombia. We also thank IPICyT-LINAN for SEM images.

## References


[1] Lazar M A, Varghese S and Nair S S 2012 *Catalysts* **2** 572
[2] Omo Ibhadon A and Fitzpatrick P 2013 *Catalysts* **3** 189
[3] Jaquotot P, Campillo A, Reinosa J J, Romero J J, Bengochea M A, Esteban-Cubillo A *et al* 2009 *Bol. Soc. Esp. Ceram.* **48** 95
[4] Pablo Abad Mejía, Carlos Mario and Restrepo R 2006 *Rev. Acad. Colomb. Cienc.* **30** 387
[5] Fujishima A, Zhang X and Tryk D 2008 *Surface Sci. Rep.* **63** 515
[6] Sakthivel S, Neppolian B, Arabindoo B, Palanichamy M and Murugesan V 2000 *J. Sci. Ind. Res.* **59** 556
[7] Okomoto K, Yamamoto Y, Tanaka H and Itaya A 1985 *Bull. Chem. Soc. Jpn.* **58** 2023
[8] Harris C and Kamat P 2009 *ACS Nano* **3** 682
[9] Augugliaro V, Palmisano L and Sclafani A 1988 *Toxicol. Environ. Chem.* **16** 89
[10] Weng T 1993 *Photocatalytic purification and treatment of water and air* (Amsterdam: Elsevier Publishers)
[11] Antonelli D M and Ying J Y 1995 *Angew. Chem. Int. Ed. Engl.* **34** 2014
[12] Miao Z, Xu D, Ouyang J, Guo G, Zhao X and Tang Y 2002 *Nano Lett.* **2** 717
[13] Terabe K, Kato K, Miyazaki H, Yamaguchi S, Imai A and Iguchi Y 1994 *J. Mater. Sci.* **29** 1617
[14] Yamagishi M, Kuriki S, Song P K and Shigesato Y 2003 *Thin Solid Films* **442** 227
[15] Pradhan S K, Bhavanasi V, Sahoo S, Sarangi S N, Anwar S and Barhai P K 2012 *Thin Solid Films* **520** 1809
[16] Yamagishia M, Kurikib S, Songa P and Shigesato Y 2003 *Thin Solid Films* **432** 227432
[17] Conde-Gallardo A, Guerrero M, Castillo N, Soto A B, Fragoso R and Cabañas-Moreno J G 2005 *Thin Solid Films* **473** 68
[18] Oja I, Mere A, Krunks M, Solterbeck C-H and Es-Souni M 2004 *Solid State Phenomena* **99–100** 259
[19] Aoki A and Nogami G 1996 *J. Electrochem. Soc.* **143** L191
[20] Kemell M, Pore V, Tupala J, Ritala M and Leskela M 2007 *Chem. Mater.* **19** 1816
[21] Aarik A, Aidla J, Uustare T and Sammelselg V 1995 *J. Crystal Growth* **148** 268
[22] Heikkilä M, Puukilainen E, Ritala M and Leskelä M 2009 *J. Photochem. Photobiol. A: Chem.* **204** 200
[23] Cho M-H, Roh Y S, Whang C N, Jeong K, Nahm S W, Ko D-H *et al* 2008 *Appl. Phys. Lett.* **81** 472
[24] Ahn C H, Cho S G, Lee H J, Park K H and Jeong S H 2001 *Metals Mater. Int.* **7** 621
[25] Lee J and Sung M 1977 *Am. Chem. Soc.* **126** 28
[26] Suntola T and Antson J 1977 *Method for producing compound thin films* Patent 4058430, November 15 1977
[27] Sathish M, Viswanathan B and Viswanath R P 2005 *Chem. Mater.* **17** 6349
[28] Jawetz E, Melnick J and Adelberg E 1995 *Microbiología Médica*. México D.F 15a Edición. Editorial EL Manual Moderno S.A de C.V. 249–263, 265-268
[29] Cho M, Chung H, Choi W and Yoon J 2005 *Appl. Environ. Microbiol.* **71** 270
[30] Chang Y-H, Liu C M, Chen C and Cheng H-E 2012 *J. Electrochem. Soc.* **159** D401
[31] Serpone N 2006 *J. Phys. Chem. B* **110** 24287
[32] Ye Cong, Jinlong Zhang, Feng Chen and Masakazu Anpo 2007 *J. Phys. Chem. C* **111** 6976
[33] Xiang Xia, Shi Xiao-Yan, Gao Xiao-Lin, Ji Fang and Wang Ya-Jun 2012 *Chin. Phys. Lett.* **29** 027801
[34] Zhang W, He Y, Yin Z and Chen Q 2000 *J. Phys. D: Appl. Phys.* **33** 912
[35] Cong Y, Zhang J, Chen F and Anpo M 2007 *J. Phys. Chem. C* **111** 6976
[36] Jakiela S, Kaminski T, Weibel D and Garsteck P 2013 *Angew. Chem. Int. Ed. Engl.* **52** 8908
[37] Verdier T, Coutand M, Berton A and Roques C 2014 *Coatings* **4** 670
[38] Rahim S and Radiman S 2012 *Sains Malaysiana* **41** 219
[39] Sangchay W 2014 *J. Nanomater. Biostruct.* **9** 1593